# Solution-Processed Aluminum Oxide Phosphate Thin-Film Dielectrics

Stephen T. Meyers,[†] Jeremy T. Anderson,[†] David Hong,[‡] Celia M. Hung,[‡] John F. Wager,[‡] and Douglas A. Keszler*,[†]

*Department of Chemistry, Oregon State University, 153 Gilbert Hall, Corvallis, Oregon 97331-4003, and School of Engineering and Computer Science, Oregon State University, Corvallis, Oregon 97331-5501*

*Received January 27, 2007. Revised Manuscript Received April 7, 2007*

Aluminum oxide phosphate thin films have been deposited via spin coating from aqueous solution and utilized as gate dielectrics in thin-film transistors. Films are atomically smooth, dense, and amorphous, while exhibiting excellent morphological stability to 1000 °C. Film chemistry and structure are investigated by using an array of analytical techniques including X-ray diffraction, FT-IR spectroscopy, and electron-microprobe analysis. Dielectric film functionality and quality are explored through integration in capacitor and thin-film transistor devices. Film permittivity for an $Al_2PO_{5.5}$ composition is found to be 4.8 in combination with leakage current densities $<10$ nA cm$^{-2}$ at 1 MV cm$^{-1}$ and current-limited breakdown fields up to 10 MV cm$^{-1}$. Thin-film transistors fabricated with these oxide phosphate dielectrics and sputtered ZnO channels exhibit strong field-effect and current saturation with incremental mobilities up to 3.5 cm$^2$ V$^{-1}$ s$^{-1}$. The ability of the amorphous matrix to accommodate additional oxide components is demonstrated by the incorporation of $La_2O_3$ and a resulting increase in film permittivity to 8.5, while maintaining breakdown fields $>4$ MV cm$^{-1}$.

## Introduction

Digital fabrication of thin-film electronics and microelectromechanical systems (MEMS) via high-speed printing of solution-processed film stacks is an attractive alternative to conventional vapor deposition, especially for ultra-low-cost and large-area applications. While much of the research in this field has focused on small-molecule and polymer-based organics, theoretical studies and all practical results to date indicate a relatively low-performance ceiling for these materials.[1−4] In contrast, inorganic materials offer potential performance several orders of magnitude higher. Indeed, promising results have been reported on the solution-phase deposition of silicon, chalcogenide, and carbon-nanotube semiconductors as transistor channels, though integration, environmental, and device-stability issues have yet to be addressed.[5−8] Given recent advances in vacuum-deposited oxide semiconductors,[9,10] stable and complementary solution-processed all-oxide devices offer a new approach, provided suitable deposition chemistries are developed. An operational solution-processed oxide gate dielectric represents a vital part of this vision, and the stringent requirements on film quality and electrical characteristics make it a challenging target and key development milestone. In this contribution, we describe the solution deposition and processing of such a high-performance gate dielectric.

Thin-film transistor (TFT) gate dielectrics must be smooth, dense, free from pinholes and charge-trapping defects and exhibit low-leakage current under applied bias. Many of these same attributes are also desirable for a wide range of applications both within and beyond traditional thin-film electronics, e.g., memory devices, passive components, and corrosion barriers. The singular importance of a superior oxide dielectric is best illustrated by the universal adoption of Si in conventional microelectronics, not for its quite ordinary semiconductor attributes, but rather for the extraordinary insulating characteristics of its native oxide.[11] The modest, bias-dependent mobilities of disordered semiconductors and high voltages encountered in contemporary thin-film devices render the need for low-leakage dielectrics even more acute for large-area applications. In fact, the lack of analogous low-cost oxide dielectrics suitable for macroarea additive processing is a major obstacle to the realization of ubiquitous macroelectronics.[12]

The chemical requirements for solution-phase deposition of homogeneous metal oxide films were suggested more than

* To whom correspondence should be addressed. E-mail: douglas.keszler@oregonstate.edu.
† Department of Chemistry.
‡ School of Engineering and Computer Science.

(1) Liu, P.; Wu, Y.; Li, Y.; Ong, B. S.; Zhu, S. *J. Am. Chem. Soc.* **2006**, *128*, 4554.
(2) Stingelin-Stutzmann, N.; Smits, E.; Wondergem, H.; Tanase, C.; Blom, P.; Smith, P.; de Leeuw, D. *Nat. Mater.* **2005**, *4*, 601.
(3) McCulloch, I.; Heeney, M.; Bailey, C.; Genevicius, K.; Macdonald, I.; Shkunov, M.; Sparrowe, D.; Tierney, S.; Wagner, R.; Zhang, W.; Chabinyc, M.; Kline, J.; McGehee, M.; Toney, F. *Nat. Mater.* **2006**, *5*, 328.
(4) Sirringhaus, H. *Adv. Mater.* **2005**, *17*, 2411.
(5) Mitzi, D. B.; Copel, M.; Chey, S. J. *Adv. Mater.* **2005**, *17*, 1285.
(6) Mitzi, D. B. *J. Mater. Chem.* **2004**, *14*, 2355.
(7) Cao, Q.; Hur, S.; Zhu, Z.; Sun, Y.; Wang, C.; Meitl, M. A.; Shim, M.; Rogers, J. A. *Adv. Mater.* **2006**, *18*, 304.
(8) Shimoda, T. T.; Matsuki, Y.; Furusawa, M.; Aoki, T.; Yudasaka, I.; Tanaka, H.; Iwasawa, H.; Wang, D.; Miyasaka, M.; Takeuchi, Y. *Nature* **2006**, *440*, 783.
(9) Nomura, K.; Ohta, H.; Takagi, A.; Kamiya, T.; Hirano, M.; Hosono, H. *Nature* **2004**, *432*, 488.
(10) Chiang, H. Q.; Wager, J. F.; Hoffman, R. L.; Jeong, J.; Keszler, D. A. *Appl. Phys. Lett.* **2005**, *86*, 013503.
(11) Greve, D. W. *Field Effect Devices and Applications*; Prentice Hall: Englewood Cliffs, NJ, 1998.

10.1021/cm0702619 CCC: $37.00 
Published on Web 07/04/2007

40 years ago.[13] Nevertheless, the aforementioned morphological constraints imposed upon a thin-film transistor (TFT) gate dielectric have proven difficult for solution-processed oxides to overcome. Common techniques using metal-organic precursors require controlled hydrolysis in combination with stabilizing ligands and organic solvents, which are typically decomposed and expelled under heat.[14] The disruptive volume loss following from these requisite high-temperature anneals often lead to discontinuities, surface roughness, and crystallization.[15] Moderate TFT performance necessitates minimal leakage current across the dielectric, rendering such defects fatal to transistor functionality. Recently, surface-mediated solution processes and layered oxide nanosheets have been advanced as means to achieve the necessary film quality for high-$\kappa$ Si applications.[16,17] In addition to unproven device integration, however, the limited growth rates, throughput, and process flexibility of these methods make them incompatible with macroarea additive processing. The approach taken in this contribution relies on fostering native $M-(OH)_x-M$ interactions within an aqueous precursor solution by controlling pH, limiting high-volume ligands and non-functional counterions, and preventing formation of large sol particles. These metastable hydroxo frameworks allow smooth, hydrated films to rapidly dehydrate through a series of hydroxide condensation reactions, forming glassy products without pore formation or cracking. Using a similar methodology, we recently reported the first practical direct deposition of an inorganic, aqueous solution processed medium-$\kappa$ oxide dielectric.[18] As a corollary to these investigations, aluminum oxide phosphate (AlPO) films of the general formula $Al_2O_{3-3x}(PO_4)_{2x}$ have been fabricated and their dielectric properties evaluated.

In many ways, aluminum is an ideal candidate metal for a solution-processed oxide dielectric because of its well-known propensity to form polymerized hydroxo networks in aqueous solution and dense amorphous oxide dielectrics via vacuum methods.[19−22] However, the direct dissolution, deposition, and hydrolytic decomposition of soluble aluminum salts generally results in poor quality oxide films. $AlPO_4$, though less polarizable than $Al_2O_3$, is interesting for its marked structural and physical similarities to $SiO_2$. Furthermore, the tendency toward polycation condensation and gel formation within aqueous $Al^{+3}-PO_4^{-3}$ systems has been well-documented,[23,24] providing evidence of the strong interactions possible in hetero-polycation solutions. In this context the use of aluminum−phosphate interactions to enhance aqueous solubility, morphology, and curing characteristics for aluminum-based films is relatively unexplored, despite its first suggestion by Rothon over 20 years ago.[25] Instead, most studies to date have used metal-organic precursors in nonaqueous pyrosol processes, delivering poor quality aluminum−phosphate films unsuitable for extensive dielectric analysis.[26−28] Here, we have used simple acidic cation hydration chemistry to design aqueous aluminum-phosphate-based hetero-polycation precursors. These solutions undergo prompt condensation with applied heat to form oxide films with morphologies and electrical performance generally possible only through expensive high-vacuum methods. Initial discussion will be directed to elucidation of the composition and atomically dense morphologies observed in AlPO films, followed by their consequent dielectric properties and seminal use in qualitatively ideal TFTs.

## Experimental Section

**Synthesis.** Precursor solutions were prepared by dissolving $Al(OH)_3$ (Alfa) in 2 mole equivalents of HCl (aq) (EMD, ACS 37%) or $HNO_3$ (aq) (Fisher, ACS 70%) (for La modifications only) and the appropriate amount of $H_3PO_4$ (aq) (Fisher, ACS 85%). $Al(OH)_3$ dissolution was accomplished by stirring under moderate heat (80−90 °C) in a water bath for 24 h. La:AlPO precursor solutions were prepared by dissolving $La_2O_3$ (Cerac 99.9%) in the preceding $HNO_3$-based solutions (up to 33% of the total metal ion concentration.) Total metal ion concentrations ranged from 0.1 to 1 M; 18 MΩ Millipore water was used for the preparation of all solutions.

**Film Preparation and Characterization.** Thin films were prepared by depositing precursor solutions on Si substrates and rotating at 3000 rpm for 30 s followed by an immediate hot-plate cure at 275 °C for 30 s. This deposition was repeated as necessary to obtain the desired thickness, and the process was completed with a furnace anneal in air at 275−1200 °C for 5−60 min. Film thickness per deposition cycle was dependent on both solution concentration and anneal temperature. Typical film thickness for one deposition cycle with a 0.5 M Al solution was ∼38 nm following an anneal at 300 °C for 30 min. Unless otherwise noted, films were placed directly into a preheated furnace for the final anneal. Dielectric films were deposited on bare, p-type Si substrates (0.008−0.016 Ω cm), for high-temperature analysis or on 500 nm Ta metal sputter deposited on Si for anneal temperatures ≤350 °C. La:AlPO dielectric films were tested on 100 nm of indium tin oxide (ITO) that was deposited via rf sputtering on Si substrates. Spectroscopy, diffraction, and chemical analyses were performed by using films deposited on 200 nm thermally grown $SiO_2$ on undoped Si substrates. All substrate surfaces were cleaned by

(12) Reuss, R. H.; Chalamala, B. R.; Moussessian, A.; Kane, M. G.; Kumar, A.; Zhang, D. C.; Rogers, J. A.; Hatalis, M.; Temple, D.; Moddel, G.; Eliasson, B. J.; Estes, M. J.; Kunze, J.; Handy, E. S.; Harmon, E. S.; Salzman, D. B.; Woodall, J. M.; Alam, M. A.; Murthy, J. Y.; Jacobsen, S. C.; Olivier, M.; Markus, D.; Campbell, P. M.; Snow, E. *Proc. IEEE* **2005**, *93*, 1239.
(13) Schroeder, H. *Phys. Thin Films* **1969**, *5*, 87.
(14) Bhuiyan, M. S.; Paranthaman, M.; Salama, K. *Supercond. Sci. Technol.* **2006**, *19*, R1.
(15) Ong, R. J.; Payne, D. A.; Sottos, N. R. *J. Am. Ceram. Soc*. **2005**, *88*, 2839.
(16) Aoki, Y.; Kunitake, T. *Adv. Mater.* **2004**, *16*, 118.
(17) Osada, M.; Ebina, Y.; Funakubo, H.; Yokoyama, S.; Kiguchi, T.; Takada, K.; Sasaki, T. *Adv. Mater.* **2006**, *18*, 1023.
(18) Anderson, J. T.; Munsee, C.; Hung, C. M.; Phung, T. M.; Johnson, D. C.; Herman, G. S.; Wager, J. F.; Keszler, D. A. *Adv. Funct. Mater.*, in press.
(19) Fu, G.; Nazer, L. F.; Bain, A. D. *Chem. Mater.* **1991**, *3*, 602.
(20) Bottero, J. Y.; Cases, J. M.; Flessinger, F.; Poirier, J. E. *J. Phys. Chem.* **1980**, *84*, 2933.
(21) Pophristic, V.; Klein, M. L.; Holerca, M. N. *J. Phys. Chem. A* **2004**, *108*, 113.
(22) Saraswati, V.; Rao, G. V. N.; Rao, G. V. R. *J. Mater. Sci.* **1987**, *22*, 2529.
(23) Lima, E. C.; Galembeck, F. *J. Colloid Interface Sci.* **1994**, *166*, 309.
(24) Montagne, L.; Palavit, G.; Draoui, M. *J. Non-Cryst. Solids* **1993**, *155*, 115.
(25) Rothon, R. N. *Thin Solid Films* **1981**, *77*, 149.
(26) Daviero, S.; Avinens, C.; Ibanez, A.; Cambie, C.; Maurin, M.; Phillipot, E. *Vide les Couches Minces* **1990**, *45*, 23.
(27) Daviero, S.; Avinens, C.; Ibanez, A.; Giuntini, J. C.; Philippot, E. *J. Non-Cryst. Solids* **1992**, *146*, 279.
(28) Daviero, S.; Ibanez, A.; Avinens, C.; Flank, A. M.; Philippot, E. *Thin Solid Films* **1993**, *226*, 207.

sonication in a 5% solution of Contrad 70 for 45 min at 45 °C followed by a thorough rinsing with 18 MΩ $H_2O$. Substrates were then subjected to a 10 min oxygen plasma ash at 10 mTorr, 5 sccm $O_2$, and 0.75 W $cm^{-2}$ prior to spin coating.

Transmission Fourier transform infrared (FT-IR) spectra were measured on thin films by using a Nicolet 5PC spectrometer with a reference spectrum collected from a bare substrate. Thin-film X-ray diffraction (XRD) data were collected by using a Rigaku RAPID diffractometer with Cu Kα radiation. Electron probe microanalysis (EPMA) was performed with a Cameca SX-50 with wavelength dispersive spectrometers and gas-flow proportional detectors with P-10 gas. O, Si, P, Cl, and Al Kα intensities were collected at accelerating voltages of 10, 15, and 20 kV and averaged over 10 positions on each sample. $SiO_2$, MgO, $Ca_{10}(PO_4)Cl_2$, and $Al_2O_3$ were used as standards. Raw intensities were corrected by a procedure detailed by Donovan and Tingle.[29] Quantitative elemental analysis was determined by comparing experimental K-ratios to simulated values using StrataGEM thin-film composition analysis software. Film surface morphology was analyzed by using a Digital Intstruments Nanocope III Multimode atomic force microscope operated in contact mode with a Veeco NP-20 SiN probe and a scan frequency of 2 Hz. A low-pass filter and a first-order plane fit were applied to all samples to limit high-frequency noise and sample tilt.

**Device Fabrication and Characterization.** Metal-insulator-metal (MIM) and metal-insulator-semiconductor (MIS) capacitor test structures were constructed by spin-coating AlPO films on conductive substrates as described above and then thermally evaporating 200 nm thick circular Al contacts via a shadow mask (0.011 $cm^2$) onto the dielectric. Relative dielectric constant and loss tangent in the frequency range 100 Hz to 1 MHz were determined by using a Hewlett-Packard 4192A impedance analyzer; measured dielectric constants varied by <5% across the stated frequency range. Leakage current and breakdown fields were assessed with a Hewlett-Packard 4140B picoammeter and a voltage ramp of 1 V $s^{-1}$.

Bottom gate thin-film transistor (TFT) test structures were fabricated by rf-sputter deposition of 40 nm ZnO semiconductor channels on the dielectric films through a shadow mask, followed by evaporation of 200 nm Al source and drain contacts also through shadow masks. ZnO was sputtered from a ceramic target under a total pressure of 5 mTorr with a 25 sccm flow rate for both $O_2$ and Ar. Dielectric/semiconductor stacks were then subjected to a 1 h postdeposition anneal at 300 °C in air prior to Al deposition. Semiconductor channel length was 100 μm, and device width was 500 μm for all reported devices. $SiO_2$ control dielectrics in MIS devices and TFTs were thermally grown to 100 nm thickness on p-type Si wafers with 30 nm of Ta and 300 nm of Au sputtered on the back side to allow an ohmic contact to the gate. TFTs were characterized in the dark with a Hewlett-Packard 4156C semiconductor parameter analyzer.

## Results and Discussion

**Morphology and Composition.** On the grounds that gate dielectric performance is heavily predicated on film morphology, a study was undertaken to determine the effect of phosphate content on film structure Films with an anhydrous composition corresponding to $Al_2O_{3-3x}(PO_4)_{2x}$ were cast from precursor solutions wherein the atomic ratio of phosphorus to aluminum ($x$) was varied from 0.25 to 1. The rapidly declining equilibrium solubility of aluminum at lower phosphoric acid concentrations prevented extension to $x <$ 0.25. Stoichiometric $AlPO_4$ consists of tetrahedrally coordinated Al and P atoms, and it exists in several polymorphs that closely resemble $SiO_2$ in structure and physical properties. AlPO films deposited from solutions where $x > \sim 0.80$ crystallized under mild heating (<275 °C when $x = 1$) to form mixed tridymite and cristobalite $AlPO_4$ phases, cf., Figure 1. The onset of crystallization was found to increase in temperature as $x$ decreased and to be highly dependent on heating rate and thermal history. Films cast from phosphate-deficient ($x < \sim 0.75$) solutions remained amorphous to X-rays indefinitely when heated at 800 °C and for >1 h at 1000 °C when ramped at 10 °C/min. Broad diffraction peaks consistent with cristobalite and tridymite $AlPO_4$, as well as α-$Al_2O_3$, are observed after 1 h at 1200 °C.

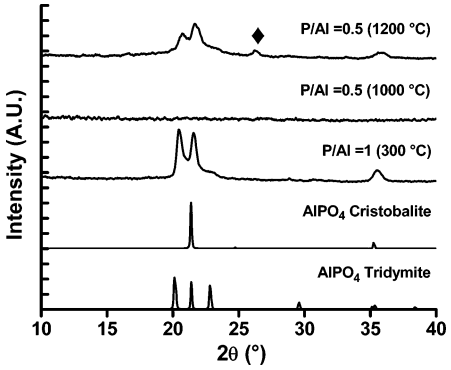


**Figure 1.** X-ray diffraction patterns of AlPO films prepared from solutions with the indicated stoichiometry annealed for 1 h following a 10 °C/min ramp. Simulated $AlPO_4$ cristobalite and tridymite patterns are included for reference. ◆ Diffraction peak at 26.3° is attributed to α-$Al_2O_3$.

The thermal stability of these amorphous oxide films is notable, even considering the relatively high activation energy commonly required for corundum nucleation from amorphous alumina. Given the high covalency of the Al−O−P matrix and the differing coordination environments for Al in $Al_2O_3$ and $AlPO_4$, this result is not entirely unexpected. Many analogous compositions consisting of covalent binary compounds substituted into more ionic and structurally dissimilar systems are known to resist film crystallization,[30−32] e.g., $SiO_2$ and $Al_2O_3$ in $HfO_2$. $P_2O_5$, though a highly covalent glass former, is not widely used in film preparation because of problematic physical vapor deposition (PVD) of the quasi-molecular oxide. Interestingly, the slow evaporation (at 100 °C) of bulk precursor solutions similar in composition ($x = 0.5$) generated powder residues that revealed significant cristobalite and tridymite content after heating at <250 °C. Presumably, the rapid condensation and strong covalent bond formation occurring in hot-plate cured thin films forestalls kinetically slower long-range diffusion and phase segregation otherwise favored during slower bulk dehydration and heating.

As in similar glasses, only limited changes in physical and optical properties have been reported in sputtered $Al_2O_3$−$AlPO_4$ films over a wide range of intermediate phosphate contents.[33,34] For this reason, and to balance the need for a

(29) Donovan, J. J.; Tingle, T. N. *J. Microsc. Soc. Am.* **1996**, *2*, 1.

(30) Nicolet, M.-A.; Giauque, P. H. *Microelectron. Eng.* **2001**, *55*, 357.
(31) Štefanić, G.; Musić, S.; Trojko, R. *J. Alloys Compd.* **2005**, *388*, 126.
(32) Neumayer, D. A.; Cartier, E. *J. Appl. Phys.* **2001**, *90*, 1801.
(33) Hanada, T.; Kano, T.; Soga, N. *Nippon Seramikkusu Kyokai Gakujutsu Ronbunshi* **1989**, *97*, 279.

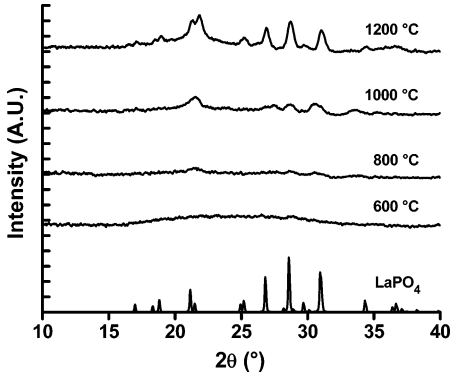


**Figure 2.** X-ray diffraction patterns of La:AlPO films prepared from solutions with a P/Al ratio of 1/2 and 33% La. Films were annealed at the indicated temperature for 1 h following a 5 °C/min ramp.

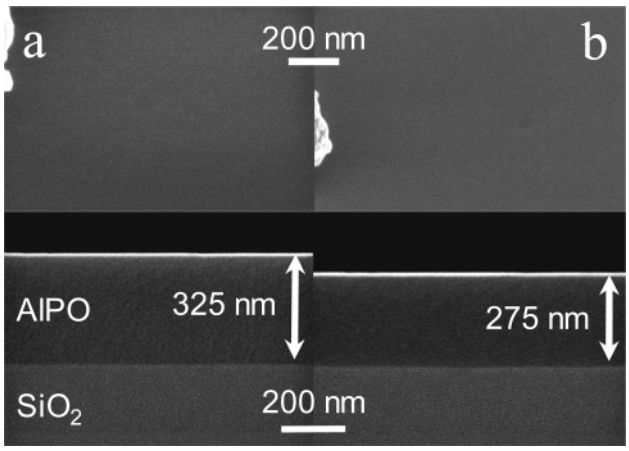


**Figure 3.** Surface and cross-sectional SEM images of an AlPO film deposited on $SiO_2$ and annealed at (a) 275 °C and (b) 600 °C. On the left of each surface image a dust particle is used as a focal point on otherwise smooth, featureless films.

thermally stable, smooth, amorphous film with a reasonable preparation time, a P/Al ratio of 1/2 was chosen as a basis for dielectric testing; further references to AlPO films herein correspond to this stoichiometry. Additionally, solutions of this composition were found to maintain sufficient acidity to accommodate dissolution of less acidic metal oxides such as $La_2O_3$, while maintaining the necessary polymerization to produce glassy films. Solutions incorporating up to 33% La relative to the total metal-ion concentration were used to fabricate dense, smooth films that remain largely amorphous after 1 h at 800 °C (Figure 2). Continued heating of La-doped films induced segregation of small-domain monoclinic $LaPO_4$ after 1 h at 1000 °C.

As seen from the scanning electron microscope (SEM) images in Figure 3, AlPO films prepared from an aqueous solution with $x = 0.5$ exhibit a dense, smooth morphology over a wide temperature range. This is noteworthy, considering the significant volume loss observed on annealing at elevated temperatures; e.g., a 15% decrease in film thickness is observed at 600 °C following an initial anneal at 275 °C. Contact-mode atomic force microscopy (AFM) imaging of identical film surfaces over a large area (25 $\mu m^2$) exposes no distinguishable features above the instrument noise floor, resulting in a root-mean-squared (RMS) roughness $\leq 0.2$ nm,

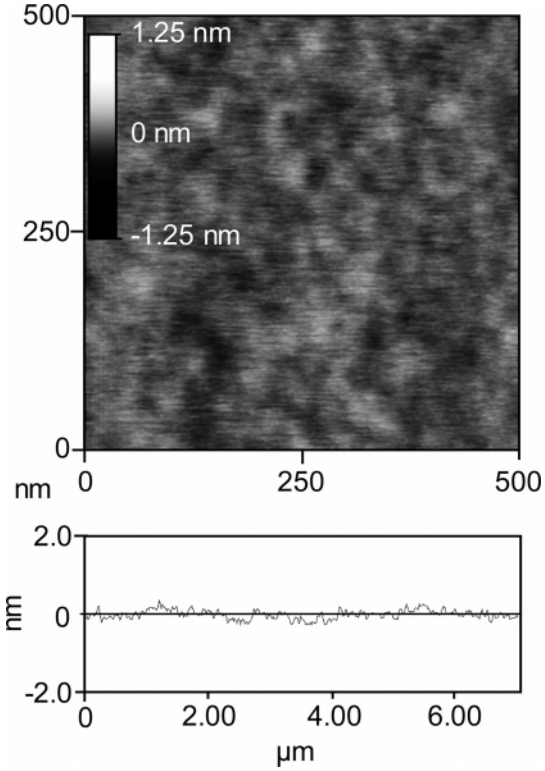


**Figure 4.** Contact-mode AFM surface and line-profile scans of an AlPO film used for dielectric testing. Film thickness is 148 nm on Si after a 1000 °C anneal for 5 min.

even for films annealed as high as 1000 °C. Higher resolution scanning across 2.5 $\mu m^2$ reveals a slight surface texture, which compares favorably to thermally grown $SiO_2$ dielectrics.[35] Typical AFM surface and 7 $\mu$m line profile scans of a 150 nm AlPO film used for electrical analysis (five deposition cycles on B-doped Si with a final anneal at 1000 °C for 5 min) are depicted in Figure 4. The maximum height variation over the surface area shown is 0.84 nm with an accompanying rms roughness of 0.08 nm.

No cracking or morphological deformation is observed through either form of microscopy, indicating that the glassy films maintain a degree of plasticity through the course of dehydration, allowing local rearrangement of bonds to relieve stresses. It has been previously noted that the strength of Al−O and P−O bonds allow a tilting or twisting of tetrahedra in the formation of bulk mesoporous glasses and zeolite-type molecular sieves in the presence of bulky organic groups,[36−38] as well as in negative thermal expansion behavior.[39] Such phenomena may also contribute to nondisruptive dehydration and densification. Inclusion of 33% La does not appreciably alter the surface roughness of films annealed up to 600 °C; rms roughness values as measured via AFM were consistently $\leq 0.2$ nm over 25 $\mu m^2$.

To confirm the volume loss associated with annealing was primarily a result of dehydration and concurrent elimination of HCl, FT-IR spectra (Figure 5) were collected from films

(34) Hanada, T.; Bessyo, Y.; Soga, N. *J. Non-Cryst. Solids* **1989**, *113*, 213.
(35) Iacona, F.; Raineri, V.; La Via, F.; Rimini, E. *J. Vac. Sci. Technol. B.* **1998**, *16*, 699.
(36) Zhang, L.; Bögershausen, A.; Eckert, H. *J. Am. Ceram. Soc.* **2005**, *88*, 897.
(37) Chen, B.; Huang, Y. *J. Am. Chem. Soc.* **2006**, *128*, 6437.
(38) Prasad, S.; Liu, S. *Chem. Mater.* **1994**, *6*, 633.
(39) Attfield, M. P.; Sleight, A. W. *Chem. Mater.* **1998**, *10*, 2013.

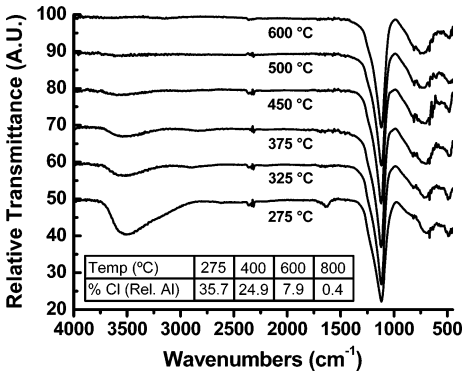


**Figure 5.** FT-IR spectra of a 183 nm AlPO film cured at the indicated temperature for 15 min. Cl content (inset) is expressed as atomic percentage relative to aluminum, as determined by EPMA.

annealed at temperatures from 275 to 600 °C. The primary features of interest are the broad absorption band centered at 3500 $cm^{-1}$ (attributed to O−H stretching modes) and the low-intensity absorption band at 1640 $cm^{-1}$ (attributed to H−O−H bending modes). Both features diminish in intensity with increasing anneal temperature, leaving no observable absorption after heating the film at 600 °C. Although slightly distorted in profile because of a necessary background correction for the $SiO_2$ layer present on the substrate, the high-intensity phosphate absorption band at 1120 $cm^{-1}$ does not decrease in intensity. $AlPO_4$ is reported to be compositionally stable under atmospheric pressure to >1500 °C, eventually decomposing into volatile $P_4O_{10}$ and $Al_2O_3$.[40] Features in the region 1000−400 $cm^{-1}$ are consistent with a superposition of Al−O and P−O vibrational modes.

Atomic percentages of Cl relative to Al from EPMA for annealed films are summarized in the inset of Figure 5. Recalling that the concentration of HCl was twice that of Al in the mother solution, it is clear that the largest fraction of Cl is eliminated during deposition and heating below 275 °C. Moreover, Cl loss is largely concurrent with dehydration in the temperature range 275−550 °C, and it is likely eliminated in the form of gaseous HCl. Films are largely free of Cl through hydrolytic decomposition (or oxidation) by 800 °C. Phosphate levels reflect those of the mother solution and remain constant (not shown) over the entire temperature range. While the lack of precision tracking of O in this case does not allow detailed dehydration information from EPMA, the nominal reaction occurring during the coating and curing of a fully dehydrated film may be expressed as

$$Al(OH)Cl_2\,(aq) + {}^1/_2H_3PO_4\,(aq) \rightarrow AlO_{3/4}(PO_4)_{1/2}\,(s) + 2HCl\,(g) + {}^1/_4H_2O\,(g)$$

**Electrical Characterization.** Electrical testing of AlPO films was performed by using two basic device structures: thin-film capacitors and field-effect transistors. Initially, MIS and MIM capacitor test structures were evaluated to provide loss tangent (tan $\delta$) and relative dielectric constant ($\epsilon_r$) values. AlPO film thicknesses were typically 135−185 nm for all devices; 100 nm thermally oxidized $SiO_2$ films were tested in identical devices for baseline analysis. A comprehensive tabulation of representative dielectric performance parameters is given in Table 1. The relative dielectric constant of ∼4.8 for AlPO films was generally independent of anneal temperature once the largest fraction of polarizeable hydroxyl groups was eliminated below 450 °C. Loss-tangent values were consistently <2% for dielectrics annealed at 300 °C and sank to <1% for dielectric films annealed at higher temperatures. Current−voltage measurements on the same devices were used for breakdown analysis of the dielectric films. As catastrophic and irreversible current increases were seldom observed in the thin-film capacitors, a current limited "breakdown" is here defined as the field strength where leakage current density equals 10 $\mu$A $cm^{-2}$. Current−voltage characteristics for AlPO films annealed over the range 300−1000 °C are illustrated in Figure 6. All films demonstrated reliable breakdown fields >5 MV $cm^{-1}$ with an increase to >7 MV $cm^{-1}$ apparent above 450 °C. Leakage current density at 1 MV $cm^{-1}$ ($J_{leak}$) was consistently <10 nA $cm^{-2}$.

Considering the change in breakdown profile observed for AlPO films on Si annealed to 1000 °C, it is possible that breakdown characteristics were modified by an underlying interfacial oxide layer formed at this temperature. Dwell times for 800 and 1000 °C anneals were limited to 10 and 5 min, respectively, to minimize interfacial oxide growth. While the effect of an interfacial $SiO_2$ layer is not clear for devices fabricated at intermediate temperatures, identical films cast on Ta substrates were found to perform similarly to those on Si after a 275 °C anneal.

**Table 1. Representative Electrical Characteristics of MIS Capacitors and TFTs with AlPO Dielectrics[a]**

| | anneal (°C) | thickness (nm) | tan $\delta$ (%) | $J_{Leak}$ (nA/$cm^2$) | $\epsilon_r$ | $\mu_{inc}$ ($cm^2$/V·s) | $V_{on}$ |
|---|---|---|---|---|---|---|---|
| AlPO (P/Al = 1/2) | 300 | 185 | 1.80 | 4.9 | 5.0 | 0.25 | −10 |
| | 450 | 170 | 1.20 | 3.0 | 4.9 | 0.35 | −6 |
| | 600 | 165 | 0.84 | 2.8 | 4.8 | 1.5 | −5 |
| | 800 | 155 | 0.80 | 2.4 | 4.8 | 3.5 | −6 |
| | 1000 | 148 | 0.55 | 0.8 | 4.8 | 3.0 | −1 |
| AlPO 33% La | 600 | 135 | 1.20 | 18.0 | 8.5 | NA | NA |
| $SiO_2$ | NA | 100 | 0.41 | 0.04 | 3.9 | 6.0 | 1 |

[a] Data from identical devices fabricated on thermally grown $SiO_2$ are included as a reference. $\mu_{inc}$ and $V_{on}$ values were taken from TFTs with ZnO channels. $J_{Leak}$ data were obtained at a field strength of 1 MV $cm^{-1}$.

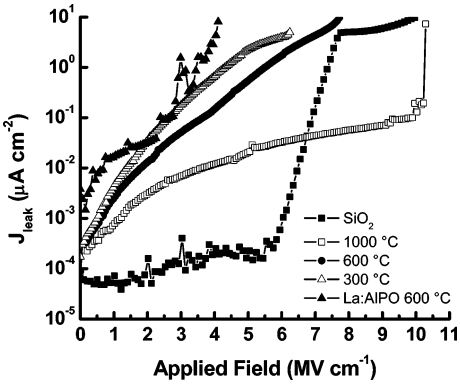


**Figure 6.** Representative current−voltage characteristics for AlPO dielectric films. Thicknesses are the same as those listed in Table 1.

(40) Wang, Z.; Danian, Y. *Dizhi Kexue* **1990**, *3*, 287.

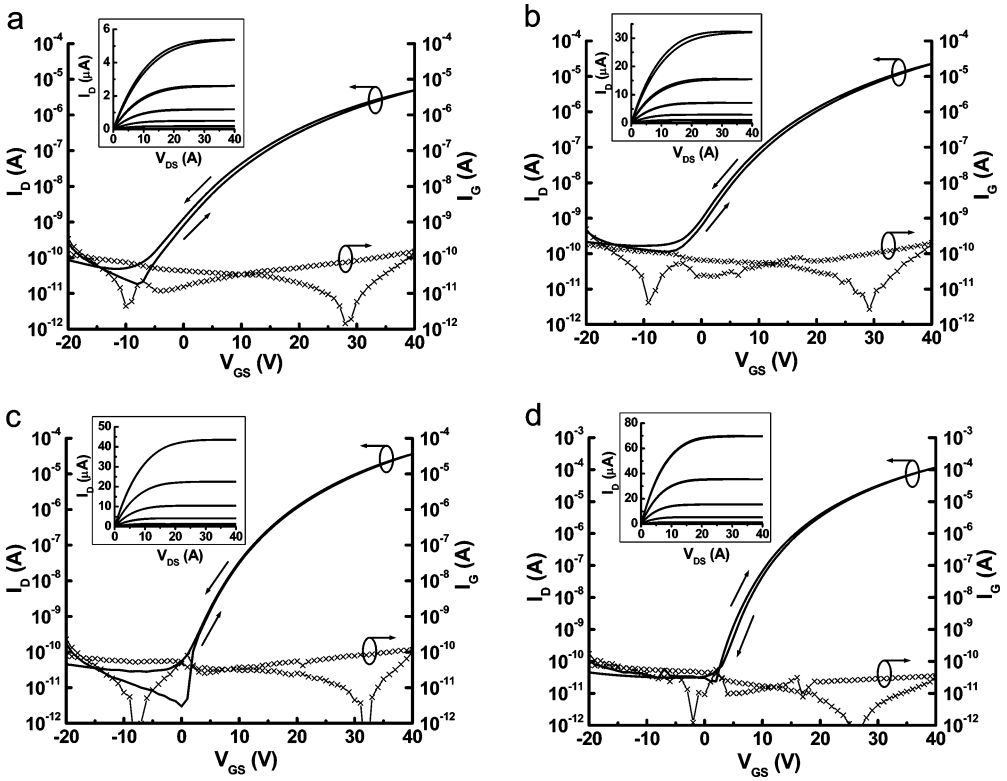


**Figure 7.** Representative $\log(I_D)-V_{GS}$ behavior ($V_{DS} = 20$ V) and (inset) $I_D-V_{DS}$ characteristics for rf-sputtered ZnO TFTs on spin-coated AlPO dielectrics annealed at (a) 300 °C, (b) 600 °C, (c) 1000 °C, and (d) thermal $SiO_2$ reference device. $V_{GS}$ is stepped from 0−40 V in 5 V increments for $I_D-V_{DS}$ curves; device $W/L$ is 5 and $L = 100$ μm.

$La_2O_3$ was dissolved in precursor solutions to produce a total La content equal to 33% of the total metal ion concentration, and thin films with this composition were deposited onto conductive ITO substrates. Dielectric analysis revealed poor breakdown characteristics at low temperatures (300 °C), possibly due to residual hydration. However, after a 30 min anneal at 600 °C La:AlPO on ITO exhibited a relative permittivity of 8.5 with associated breakdown fields >4 MV $cm^{-1}$. The loss tangent (∼1.2%) was slightly increased in comparison with standard AlPO compositions with $J_{leak}$ increasing to ∼18 nA $cm^{-2}$. Although only limited electrical characterization has so far been done on this and other modified AlPO compositions, these results indicate that the dielectric constant of glassy AlPO derivative films is tunable by a facile incorporation of other polarizable oxides. This is notable given that the dielectric parameter control offered by the $Al_2O_3-AlPO_4$ composition itself is minimal. In a similar vein, the strong bonding properties of bulk $Al_2O_3-P_2O_5$ glasses have been reported to accommodate a variety of less acidic oxides, including $La_2O_3$.[41]

Field-effect thin-film transistors with AlPO gate dielectrics were fabricated and tested with rf-sputtered ZnO active channels. TFT performance is assessed through an analysis of the turn-on voltage ($V_{on}$), drain current on-to-off ratio ($I_{on}/I_{off}$), and incremental channel mobility ($\mu_{inc}$).[42] These values afford useful figures of merit provided that qualitative TFT operation is achieved, including drain current ($I_D$) saturation with increasing drain-source voltage ($V_{DS}$), minimal hysteresis, and strong current modulation under moderate gate bias. $\mu_{inc}$ values, calculated at 40 $V_{GS}$ and 1 $V_{DS}$, are quantitatively equivalent to field-effect values and describe the mobility of carriers as they are incrementally added to the channel.

Representative characteristics for bottom-gate ZnO TFTs with AlPO gate dielectrics annealed at 300, 600, and 1000 °C, as well as thermally grown $SiO_2$ dielectrics, are shown in Figure 7. Strong gate modulation is apparent throughout the temperature range tested; drain current $I_{on}/I_{off}$ ratios range from $\sim 10^5$ to $10^6$ as dielectric anneal temperature is increased. The magnitude of the drain current and semiconductor channel mobility increase gradually with dielectric anneal temperature, presumably because of an improved interface. Interestingly, the gate leakage current ($I_{GS}$) does not appear to be significantly dependent on anneal temperature, suggesting that the overall quality of the films is not markedly changed. AlPO TFTs commonly exhibited gate leakage of 0.1−1 nA, while control $SiO_2$ devices were approximately 1 order of magnitude lower. It should be noted that the bottom gate electrode is not patterned for ease of processing, leading to a slightly elevated gate leakage for all devices. Mobility and current drive of AlPO TFTs were less than those observed for thermally grown $SiO_2$ dielectrics under all conditions. Comparable shifts in device mobility and $V_{on}$ have been previously observed when comparing various PVD dielectrics in TFTs with ZnO channels.[43,44] Clockwise hysteresis in ZnO channel TFTs has also been

(41) Karabulut, M.; Metwalli, E.; Brow, R. K. *J. Non-Cryst. Solids* **2001**, *283*, 211.
(42) Hoffman, R. L. *J. Appl. Phys.* **2004**, *95*, 5813.
(43) Carcia, P. F.; McLean, R. S.; Reilly, M. H. *J. Soc. Inf. Display* **2005**, *13*, 547.
(44) Carcia, P. F.; McLean, R. S.; Reilly, M. H. *Appl. Phys. Lett.* **2006**, *88*, 123509.

frequently reported on a variety of dielectrics, even ostensibly identical materials deposited by different methods. These effects are commonly attributed to a large density of electron-trapping defects of various energies at the semiconductor/insulator interface, and in Figure 7d a minimal amount of such hysteresis is evident in the $SiO_2$ device operation. In contrast, an opposite, counterclockwise hysteresis is observed for AlPO devices annealed at low and intermediate temperatures (Figure 7a,b). In this case, the drain current on the reverse $V_{GS}$ sweep is larger than that of the forward sweep, and a negative shift of ~2 V in $V_{on}$ is observed. This effect diminishes gradually with increasing dielectric anneal temperature, and such hysteresis is negligible (even compared to $SiO_2$) for dielectric films heated above 800 °C, as demonstrated in Figure 7c. Nearly identical behavior has been reported for ZnO devices fabricated on thick $Al_2O_3$ dielectrics deposited by electron-beam evaporation,[44] and similar effects have also been characterized in MOSFET devices with $SiO_2$ gate dielectrics.[45] In the $SiO_2$ case these effects have been attributed to mobile charges associated with hydrogen impurities (protons) migrating via a hopping mechanism on bridging O atoms to the semiconductor/dielectric interface under the application of a positive potential to the gate. Given that the complete dehydration of AlOOH and $Al_2O_3$ species has been reported to require $T \geq 1200$ °C,[22] it is probable that sufficient hydroxyl bridges are present within the mixed network of acidic phosphate/alumina tetrahedra to allow a similar migration of protons even after a moderately high temperature anneal. The presence of large numbers of O-bound protons in AlPO films at moderate temperatures is obvious from the FT-IR spectra presented above, and given the thickness of the films in question (<200 nm), a substantive degree of hydration may be expected at temperatures well above that where significant IR absorption is observed. The hydrated character of the initially smooth dielectric film is also likely to facilitate increased chemical interaction and diffusion during postdeposition anneals of the semiconductor. The ensuing interface is less abrupt and more likely to contain a large number of charge-trapping defects, resulting in the observed trends in mobility and drive current.

(45) Devine, R.; Vanheusden, K.; Herrera, G. V. *Appl. Phys. Lett.* **2000**, *77*, 579.

## Conclusion

The exceptional morphology and thermal stability exhibited by AlPO dielectric films described herein provides further evidence that appropriately tailored aqueous, all-inorganic precursor solutions offer a practical route to solution deposition of dense homogeneous oxides. In these systems the prompt condensation of polymeric hydroxocations present within the as-deposited solution facilitates the rapid formation of a robust bond network, which in turn provides a kinetic barrier to particle segregation and inhomogeneities, allowing the nondisruptive elimination of solvent molecules. In the case of AlPO precursor solutions this framework is provided by formation of aluminum−phosphate-based heteropolycations. The viability of this approach has been demonstrated by the deposition of smooth, atomically dense dielectric films with relative dielectric constants of 4.8 and the fabrication of qualitatively ideal ZnO-channel TFTs employing 148−185 nm AlPO gate dielectrics. These TFTs boast leakage currents <1 nA and incremental mobilities of 3.5 $cm^2\ V^{-1}\ s^{-1}$. This performance, realized through simple, low-cost aqueous chemistries, is tolerant of aggressive thermal processing in excess of 1000 °C because of the high stability of the glassy AlPO network. Furthermore, use of the Al−O−P matrix as a tunable amorphous host for other oxides has been demonstrated by the incorporation of $La_2O_3$ into dielectric films with a consequent enhancement in dielectric constant.

**Acknowledgment.** This work was supported by the Hewlett Packard Company and the Defense Advanced Research Projects Agency (MEMS/NEMS: Science and Technology Fundamentals). S.T.M. and D.H. were supported as IGERT fellows by the National Science Foundation under grant no. 0549503.

CM0702619